Genetics of Variable Disease Expression Conferred by Inverse Gene-For-Gene Interactions in the Wheat-*Parastagonospora nodorum* Pathosystem[1]

Amanda R. Peters Haugrud,[a,2] Zengcui Zhang,[b] Jonathan K. Richards,[c,3] Timothy L. Friesen,[b,c] and Justin D. Faris[b,4]

[a]Department of Plant Sciences, North Dakota State University, Fargo, North Dakota 58102
[b]United States Department of Agriculture-Agriculture Research Service, Cereal Crops Research Unit, Eduard T. Schafer Agricultural Research Center, Fargo, North Dakota 58102
[c]Department of Plant Pathology, North Dakota State University, Fargo, North Dakota 58102

ORCID IDs: 0000-0001-5634-2200 (T.L.F.); 0000-0002-9653-3287 (J.D.F.).

The wheat-*Parastagonospora nodorum* pathosystem involves the recognition of pathogen-secreted necrotrophic effectors (NEs) by corresponding wheat NE sensitivity genes. This inverse gene-for-gene recognition leads to necrotrophic effector-triggered susceptibility and ultimately septoria nodorum blotch disease. Here, we used multiple pathogen isolates to individually evaluate the effects of the host gene-NE interactions *Tan spot necrosis1*-Stagonospora nodorum ToxinA (*Tsn1*-SnToxA), *Stagonospora nodorum necrosis1*-Stagonospora nodorum Toxin1 (*Snn1*-SnTox1), and *Stagonospora nodorum necrosis3-B genome homeolog1*-Stagonospora nodorum Toxin3 (*Snn3-B1*-SnTox3), alone and in various combinations, to determine the relative importance of these interactions in causing disease. Genetic analysis of a recombinant inbred wheat population inoculated separately with three *P. nodorum* isolates, all of which produce all three NEs, indicated that the *Tsn1*-SnToxA and *Snn3-B1*-SnTox3 interactions contributed to disease caused by all four isolates, but their effects varied and ranged from epistatic to additive. The *Snn1*-SnTox1 interaction was associated with increased disease for one isolate, but for other isolates, there was evidence that this interaction inhibited the expression of other host gene-NE interactions. RNA sequencing analysis in planta showed that *SnTox1* was differentially expressed between these three isolates after infection. Further analysis of NE gene-knockout isolates showed that the effect of some interactions could be masked or inhibited by other compatible interactions, and the regulation of this occurs at the level of NE gene transcription. Collectively, these results show that the inverse gene-for-gene interactions leading to necrotrophic effector-triggered susceptibility in the wheat-*P. nodorum* pathosystem vary in their effects depending on the genetic backgrounds of the pathogen and host, and interplay among the interactions is complex and intricately regulated.

Wheat (*Triticum aestivum*) currently supplies 20% of the world's calorie intake. *Parastagonospora* (syn. *ana, Stagonospora; teleo, Phaeosphaeria*) *nodorum* (Berk.) Quaedvleig, Verkley, and Crous is a necrotrophic fungal pathogen that causes the disease septoria nodorum blotch (SNB; formerly called Stagonospora nodorum blotch). SNB can lead to severe yield losses, reaching upwards of 50% (Eyal et al., 1987), and decrease grain quality.

Biotrophic pathogens require living tissue to proliferate and complete their life cycle. Plants have innate immune systems to combat biotrophic pathogens that involve the recognition of pathogen-produced molecules, such as effectors and pathogen-associated molecular patterns (PAMPs). Recognition of PAMPs, which are usually conserved molecules that serve essential functions, occurs by way of pattern recognition receptors (PRRs) in the host and leads to the activation of the PAMP-triggered immunity (PTI) pathway characterized by an oxidative burst, activation of defense response genes, and sometimes localized cell death (Jones and Dangl, 2006; Day et al., 2011; van Schie and Takken, 2014). Recognition of pathogen-produced effectors by plant resistance genes occurs in a gene-for-gene manner (Flor, 1956). This recognition leads to activation of the effector-triggered immunity (ETI) pathway and provides a second layer of defense against biotrophic pathogens. The ETI responses largely overlap with those of the PTI pathway resulting in the restriction of biotrophic pathogen growth (van Schie and Takken, 2014).

[1]This work was supported by the U.S. Department of Agriculture (USDA) Agriculture and Food Research Initiative Competitive (Grant 2015-67012-23221).

[2]Senior author.

[3]Present address: Department of Plant Pathology and Crop Physiology, Louisiana State University Agricultural Center, Baton Rouge, Louisiana 70803.

[4]Author for contact: justin.faris@ars.usda.gov.

The author responsible for distribution of materials integral to the findings presented in this article in accordance with the policy described in the Instructions for Authors (www.plantphysiol.org) is: Justin D. Faris (justin.faris@ars.usda.gov).

A.R.P.H. and Z.Z. performed the experiments; A.R.P.H., J.K.R., T.L.F., and J.D.F. designed the experiments and analyzed the data; A.R.P.H. and J.D.F. wrote the manuscript with contributions from all authors; T.L.F. and J.D.F. conceived the research project.

www.plantphysiol.org/cgi/doi/10.1104/pp.19.00149

Necrotrophic pathogens like *P. nodorum* induce cell death by secreting necrotrophic effectors (NEs) that, when recognized by the host, elicit the activation of programmed cell death and other components of the host defense response (Friesen and Faris, 2010; Winterberg et al., 2014; Shi et al., 2016b). However, because the pathogen can survive the various components of this defense response and feed on the dying cells, the result is host susceptibility (pathogen virulence). Therefore, these interactions are referred to as "inverse gene-for-gene" because the recognition of NEs by dominant host sensitivity genes leads to necrotrophic effector triggered susceptibly (NETS) as opposed to ETI as is observed in host-biotroph gene-for-gene interactions (Friesen and Faris, 2010; Oliver et al., 2012; Shi et al., 2016b).

To date, a total of nine host sensitivity gene-NE interactions have been characterized in this pathosystem: *Tan spot necrosis1 (Tsn1)*-Stagonospora nodorum ToxinA (SnToxA; Friesen et al., 2006, 2009; Liu et al., 2006; Faris and Friesen, 2009; Zhang et al., 2009; Faris et al., 2010, 2011), *Stagonospora nodorum necrosis1 (Snn1)*-Stagonospora nodorum Toxin1 (SnTox1; Liu et al., 2004b, 2004a, 2012; Reddy et al., 2008; Shi et al., 2016b), *Stagonospora nodorum necrosis2 (Snn2)*-Stagonospora nodorum Toxin2 (SnTox2; Friesen et al., 2007, 2009; Zhang et al., 2009), *Stagonospora nodorum necrosis3-B genome homeolog1 (Snn3-B1)*-Stagonospora nodorum Toxin3 (SnTox3; Friesen et al., 2008; Liu et al., 2009; Shi et al., 2016a), *Stagonospora nodorum necrosis3-D genome homeolog1 (Snn3-D1)*-SnTox3 (Zhang et al., 2011), *Stagonospora nodorum necrosis4 (Snn4)*-Stagonospora nodorum Toxin4 (SnTox4; Abeysekara et al., 2009, 2012), *Stagonospora nodorum necrosis5 (Snn5)*-Stagonospora nodorum Toxin5 (SnTox5; Friesen et al., 2012), *Stagonospora nodorum necrosis6 (Snn6)*-Stagonospora nodorum Toxin6 (SnTox6; Gao et al., 2015), and *Stagonospora nodorum necrosis7 (Snn7)*-Stagonospora nodorum Toxin7 (SnTox7; Shi et al., 2015).

The *Tsn1*-SnToxA, *Snn1*-SnTox1, and *Snn3-B1*-SnTox3 interactions have been studied more intensively due to the cloning of host sensitivity and/or pathogen NE genes. The NE SnToxA interacts with the wheat sensitivity gene *Tsn1*, which encodes a protein consisting of an N-terminal Ser/Thr protein kinase domain and C-terminal nucleotide binding and Leu-rich repeat domains (Friesen et al., 2006; Faris et al., 2010). The *ToxA* gene is unique compared with the other NEs in the wheat-*P. nodorum* system in that it was likely horizontally transferred to *Pyrenophora tritici-repentis* (Friesen et al., 2006) and has recently been identified in *Bipolaris sorokiniana* (Friesen et al., 2018; McDonald et al., 2018) and *Cochliobolus heterostrophus* (Lu et al., 2015), making ToxA an important virulence factor for multiple host-pathogen interactions.

The *Snn3-B1*-SnTox3 interaction has been shown to contribute significantly to SNB in some host genetic backgrounds (Friesen et al., 2008). *Snn3-B1* is located on the short arm of chromosome 5B, and fine mapping has been done to initiate the cloning process (Shi et al., 2016a). *SnTox3* was cloned by Liu et al. (2009) and encodes for a secreted protein. After recognition, host defense genes are up-regulated leading to programmed cell death. However, these host genes differ from those associated with the *Tsn1*-SnToxA interaction (Winterberg et al., 2014).

Snn1 is located on the short arm of chromosome 1B (Liu et al., 2004b) and was cloned by Shi et al. (2016b). The *Snn1* gene product is a wall-associated kinase protein that is similar in structure to PRR proteins typically involved in early recognition of pathogens and the up-regulation of the PTI pathway. *Snn1* was the first susceptibility gene to be cloned with a PRR-like structure, suggesting that necrotrophic pathogens have evolved the ability to hijack both the PTI and the ETI pathways. *SnTox1* was cloned by Liu et al. (2012) and encodes a protein that is Cys-rich and contains a functional chitin-binding motif. SnTox1 is unique from other known NEs in that it is a dual-function protein (Liu et al., 2016). SnTox1 binds chitin and protects the pathogen from wheat chitinases (Liu et al., 2016) in addition to interacting directly with the Snn1 protein (Shi et al., 2016b). The important role SnTox1 plays in penetration, colonization, and sporulation may be the reason that ~95.4% of the U.S. *P. nodorum* natural population and 84% of *P. nodorum* isolates worldwide carry *SnTox1* (T. L. Friesen and J. K. Richards, unpublished data), which is much higher than the frequency of *Snn1* in wheat (McDonald et al., 2013).

It has been shown that when multiple interactions occur between wheat and *P. nodorum*, there is a higher level of disease severity with the interactions contributing additively to overall disease (as reviewed by Friesen and Faris, 2010). Variable expression of NE genes also contributes to disease severity and adds another layer of complexity to the wheat-*P. nodorum* pathosystem. Faris et al. (2011) found that increased *SnToxA* expression in the *P. nodorum* isolate BBC03Sn5 compared with LDN03Sn4 led to the *Tsn1*-SnToxA interaction contributing to a higher level of disease in BBC03Sn5 than LDN03Sn4. Gao et al. (2015) found that, despite the presence of the *SnTox1* gene in the isolate Sn6, the *Snn1*-SnTox1 interaction was not a significant contributor to disease due to the lack of *SnTox1* transcription. Recently, Phan et al. (2016) found that when *SnTox1* is eliminated from the isolate SN15, *SnTox3* expression is increased, implying that *SnTox1* may suppress *SnTox3*. Although multiple studies have looked at *SnTox1* expression in single isolates, no research has been published comparing *SnTox1* expression across multiple *P. nodorum* isolates on a single host population.

The cloning of the three NE genes *SnToxA*, *SnTox1*, and *SnTox3* makes it feasible to dissect and quantify the relative effects of the *Tsn1*-SnToxA, *Snn1*-SnTox1, and *Snn3-B1*-SnTox3 interactions, but their effects have not been evaluated in a single host genetic background. Here, we evaluated multiple *P. nodorum* isolates that produce all three NEs for their ability to cause SNB, and quantified the roles of each compatible interaction in

causing disease. We show that the roles of these interactions in contributing to SNB vary depending on the isolate, and that relationships can range from additive to epistatic, with even some evidence of antagonistic effects of one interaction leading to inhibition of others. Our results suggest that a transcriptionally regulated balance of NE production is maintained in *P. nodorum*.

RESULTS

Marker Analysis and Linkage Map Construction

A population of 190 recombinant inbred lines (RILs) derived from a cross of the common hexaploid wheat line Sumai 3 and a Chinese Spring–*Triticum turgidum* ssp. *dicoccoides* chromosome 5B disomic chromosome substitution line (CS-DIC 5B), hereafter referred to as the CDS population, was developed and genotyped with simple sequence repeat (SSR) and single nucleotide polymorphism (SNP) markers to generate genetic linkage maps representing the whole genome. The maps consisted of 98 SSRs, 2,098 SNPs, and the three NE sensitivity gene loci (*Tsn1*, *Snn1*, and *Snn3-B1*; see below), for a total of 2,199 markers including 848 unique loci (Supplemental Table S1). The maps were used to quantify the effects of the NE sensitivity loci using quantitative trait loci (QTL) analysis methods.

Genetic Analysis and Mapping of the NE Sensitivity Genes *Tsn1*, *Snn3-B1*, and *Snn1*

CS-DIC 5B carries *Snn1* but not *Tsn1* or *Snn3-B1*; therefore, it was sensitive to SnTox1 but not SnToxA or SnTox3 (Fig. 1). Sumai 3 harbors *Tsn1* and *Snn3*-B1 but lacks *Snn1* and was therefore sensitive to SnToxA and SnTox3 but insensitive to SnTox1. The segregation ratios and χ^2 analysis of the NE reactions in the CDS population are presented in Supplemental Table S2. The NE sensitivity genes *Tsn1*, *Snn3-B1*, and *Snn1* mapped to chromosome arms 5BL, 5BS, and 1BS, respectively (Supplemental Table S1), as expected.

Analysis of Inverse Gene-For-Gene Interactions using *P. nodorum* Isolates that Produce All Three NEs

The *P. nodorum* isolates Sn4, Sn5, and SN15, all of which are known to harbor the *SnToxA*, *SnTox1*, and *SnTox3* genes, were inoculated onto the CDS population to evaluate the relative effects of compatible *Tsn1*-SnToxA, *Snn1*-SnTox1, and *Snn3-B1*-SnTox3 interactions in causing SNB. At least three replications of inoculations for each isolate were conducted, and Bartlett's χ^2 tests for homogeneity between replicates within each isolate indicated that the variance among the replicates was not significantly different (Supplemental Table S3). Therefore, mean reaction type scores for each isolate were used for further analysis. The reaction types were obtained using the 0–5 lesion type scale, where 0 = highly resistant and 5 = highly susceptible, as defined in Liu et al. (2004b).

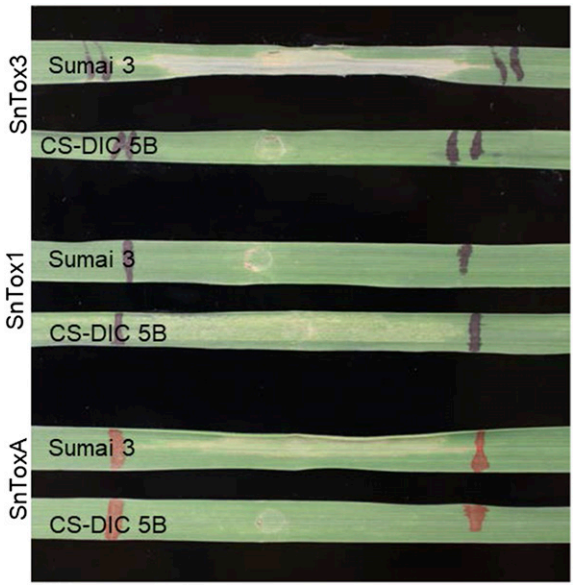

Figure 1. Leaves of Sumai 3 and CS-DIC 5B infiltrated with SnTox3, SnTox1, and SnToxA. Sumai 3 is sensitive to SnTox3 and SnToxA and insensitive to SnTox1, whereas CS-DIC 5B is sensitive to SnTox1 and insensitive to SnTox3 and SnToxA.

P. nodorum *Isolate Sn4*

For Sn4, CS-DIC 5B had an average reaction type score of 2.10 (moderately resistant) and Sumai 3 had an average score of 3.80 (susceptible; Fig. 2; Tables 1 and 2; Supplemental Fig. S1). The average reaction type score for the CDS population was 2.96, and individuals in the population had average reaction types that ranged from 1.38 to 4.00 (Table 1; Supplemental Fig. S1).

To analyze the effects of different combinations of the interactions together and individually, the 118 RILs were divided into eight genotypic classes based on their allelic compositions at the *Tsn1*, *Snn1*, and *Snn3-B1* loci (Table 2). The reaction type mean for lines with *Snn1* as the only NE sensitivity gene (*Snn1/snn3-B1/tsn1* lines) was not significantly different from lines with no NE sensitivity genes (*snn1/snn3-B1/tsn1*), suggesting that the *Snn1*-SnTox1 interaction did not significantly contribute to disease caused by Sn4. However, lines with only *Tsn1* (*snn1/snn3-B1/Tsn1*) and lines with only *Snn3-B1* (*snn1/Snn3-B1/tsn1*) were significantly more susceptible than lines containing no NE sensitivity genes (*snn1/snn3-B1/tsn1*), but the reaction type means for SnTox3 and/or SnToxA sensitive lines (lines with *Snn3-B1* and/or *Tsn1*) were not significantly different from each other ($P < 0.05$). These results suggest that the *Tsn1*-SnToxA and *Snn3-B1*-SnTox3 interactions played significant roles in SNB caused by Sn4, but their effects were not additive because the presence of both *Snn3-B1* and *Tsn1* did not make plants

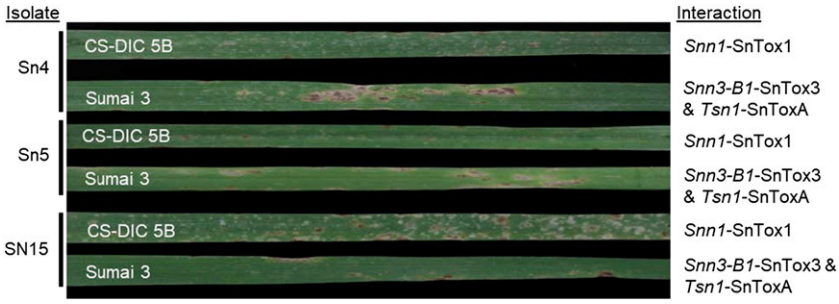

Figure 2. Leaves of CS-DIC 5B and Sumai 3 inoculated with different *Parastagonospora nodorum* isolates. CS-DIC 5B has the NE sensitivity gene *Snn1*, whereas Sumai 3 has *Snn3-B1* and *Tsn1*. *P. nodorum* isolates Sn4, Sn5, and SN15 contain the NE genes *SnTox1*, *SnTox3*, and *SnToxA*.

significantly more susceptible than plants with one of the two genes.

A second method of analyzing the effects of compatible interactions was conducted using the QTL identification approach known as composite interval mapping (CIM). Analysis of SNB reaction type means caused by Sn4 indicated that the *Snn3-B1* and *Tsn1* loci were both significantly associated with SNB susceptibility (Fig. 3; Table 3). The *Snn3-B1* locus had a logarithm of the odds (LOD) of 4.17 and explained 17.3% of the disease variation, and *Tsn1* had a LOD of 4.13 and explained 19.2% of the disease variation. The *Snn1* locus was not significantly associated with reaction to Sn4, which agreed with the average reaction type analysis of the different genotypic combinations (Table 2).

P. nodorum *Isolate Sn5*

CS-DIC 5B and Sumai 3 had average disease reaction scores of 1.25 (resistant) and 3.25 (susceptible) to Sn5, respectively (Fig. 2; Tables 1 and 2; Supplemental Fig. S1). The CDS population had an average reaction score of 2.80 with individuals in the population ranging from 1.13 to 4.00 (Table 1; Supplemental Fig. S1).

Analysis of the reaction type means of the eight genotypic classes revealed the *Snn1/snn3-B1/tsn1* lines were not significantly different in their reaction to Sn5 compared with the lines with none of the NE sensitivity genes (*snn1/snn3-B1/tsn1*) indicating that, as with Sn4, the *Snn1*-SnTox1 interaction did not play a significant role in the development of SNB (Table 2). However, lines with only *Tsn1* (*snn1/snn3-B1/tsn1*) or only *Snn3-B1* (*snn1/Snn3-B1/tsn1*) were significantly more susceptible than the *snn1/snn3-B1/tsn1* lines, and lines containing only *Tsn1* were significantly more susceptible than lines with only *Snn3-B1*. However, in the presence of *Snn1*, lines with either *Tsn1* or *Snn3-B1* were not significantly different. In addition, lines with *Snn3-B1* and *Tsn1* but not *Snn1* (*snn1/Snn3-B1/Tsn1*) were significantly more susceptible than lines with all three NE sensitivity genes. These results suggest that, like Sn4, the *Snn3-B1*-SnTox3 and *Tsn1*-SnToxA interactions play significant roles in SNB development, and the *Snn1*-SnTox1 interaction does not. However, the role of *Snn1*-SnTox1 is more complicated in Sn5 and may contribute to resistance, or suppression of susceptibility, in the presence of some other interactions.

CIM analysis indicated that both *Tsn1* and *Snn3-B1* were significantly associated with SNB susceptibility (Fig. 3; Table 3). *Tsn1* had a LOD of 9.59 and explained 32.4% of the disease variation, whereas *Snn3-B1* had a LOD of 5.27 and explained 20.4% of the disease variation.

P. nodorum *Isolate SN15*

CS-DIC 5B and Sumai 3 had average disease reaction scores of 2.00 (moderately resistant) and 2.67 (moderately susceptible) to SN15, respectively (Fig. 2; Tables 1 and 2; Supplemental Fig. S1). The CDS population had an average disease score of 2.32, and average disease scores ranged from 0.50 to 4.50 (Table 1; Supplemental Fig. S1).

RILs containing at least one NE gene were significantly more susceptible to SN15 than lines with none of the NE sensitivity genes (*snn1/snn3-B1/tsn1*), indicating that all three interactions played significant roles in the development of SNB (Table 2). However, lines with both *Snn3-B1* and *Tsn1*, but not *Snn1* (*snn1/Snn3-B1/Tsn1*), were as susceptible as lines with all three NE sensitivity genes, and lines with *Snn1* in addition to one other NE sensitivity gene (*Snn1/Snn3-B1/tsn1* and *Snn1/snn3-B1/Tsn1*) were not significantly different from lines with only a single NE sensitivity gene. This indicated that the *Tsn1*-SnToxA and *Snn3-B1*-SnTox3

Table 1. *Average lesion-type reactions of the parental lines CS-DIC 5B and Sumai 3, along with the CDS population average and range to* P. nodorum *isolates Sn4, Sn5, SN15, Sn2000, and Sn2000KO6-1*

Isolate	CS-DIC 5B	Sumai3	Population Average	Population Range
Sn4 (*SnTox1*, *SnTox3*, *SnToxA*)	2.10	3.80	2.96	1.38-4.00
Sn5 (*SnTox1*, *SnTox3*, *SnToxA*)	1.25	3.25	2.80	1.13-4.00
SN15 (*SnTox1*, *SnTox3*, *SnToxA*)	2.00	2.67	2.32	0.50-4.50
Sn2000 (*SnTox1*, *SnToxA*)	2.00	2.56	2.24	0.06-4.07
Sn2000KO6 (*SnTox1*)	2.10	0.60	2.02	0.00-4.00

Table 2. *The different genotypic classes in the CS-DIC 5B × Sumai 3 recombinant inbred population and their average reaction score to the* P. nodorum *isolates Sn4, Sn5, and SN15*

Genotype[a]	No. RIL	Sn4 Average Reaction Type[b]	Sn5 Average Reaction Type	SN15 Average Reaction Type
CS-DIC 5B	—[c]	2.00 ± 0.41	1.25 ± 0.29	2.00 ± 0.25
Sumai 3	—	3.63 ± 0.38	3.25 ± 0.29	2.67 ± 0.29
Snn1/Snn3-B1/Tsn1	14	3.18a	3.04bcd	2.53ab
snn1/snn3-B1/tsn1	13	2.30b	2.09e	1.08d
Snn1/Snn3-B1/tsn1	18	3.07a	2.88cd	2.47bc
Snn1/snn3-B1/Tsn1	9	3.32a	3.08bc	2.46bc
Snn1/snn3-B1/tsn1	17	2.41b	1.98e	2.12c
snn1/Snn3-B1/tsn1	15	2.97b	2.76d	2.24bc
snn1/Snn3-B1/Tsn1	24	3.34a	3.39a	2.92a
snn1/snn3-B1/Tsn1	8	3.02a	3.20ab	2.20bc
$LSD_{0.05}$	—	0.39	0.29	0.40

[a]For clarity, gene symbols in bold represent the NE sensitivity allele. [b]Numbers followed by the same letter in the same column are not significantly different at the 0.05 level of probability. [c]—, Nonapplicable

interactions played significant roles and their effects were additive, but the *Snn1*-SnTox1 interaction was associated with SNB development only in the absence of the other two interactions.

CIM analysis showed that *Tsn1* and *Snn3-B1*, but not *Snn1*, were significantly associated with SNB susceptibility (Fig. 3; Table 3). *Snn3-B1* had a LOD of 5.58 and explained 20.7% of the disease variation, whereas *Tsn1* had a LOD of 4.43 and explained 17.1% of the disease variation.

Analysis of Interactions using *P. nodorum* Isolate Sn2000 and an Sn2000 *SnToxA*-Knockout Mutant

The CDS population was evaluated for reaction to SNB caused by *P. nodorum* isolate Sn2000, which contains the NE genes *SnTox1* and *SnToxA* (Liu et al., 2004b, 2012). CS-DIC 5B and Sumai 3 had average disease reaction types of 2.00 (moderately resistant) and 2.56 (moderately susceptible), respectively (Fig. 4; Tables 1, 4, and 5; Supplemental Fig. S2). The CDS population had an average reaction type of 2.24 and a population range of 0.06 to 4.07 (Table 1; Supplemental Fig. S2).

Analysis of the reaction type means of the four genotypic classes revealed that lines containing at least one NE sensitivity gene (*Tsn1* and/or *Snn1*) were significantly more susceptible to Sn2000 than lines containing neither of the NE sensitivity genes (*snn1/tsn1*), indicating that both the *Snn1*-SnTox1 and *Tsn1*-SnToxA interactions play a significant role in the development of SNB (Table 4). Lines with only *Tsn1* were significantly more susceptible than lines with only *Snn1*, indicating that the *Tsn1*-SnToxA interaction played a more significant role than the *Snn1*-SnTox1 interaction. Lines with either *Tsn1* or *Snn1* were not significantly different than lines with both genes (*Snn1/Tsn1*) indicating that the additive effects of these two interactions were not significant in SNB caused by Sn2000.

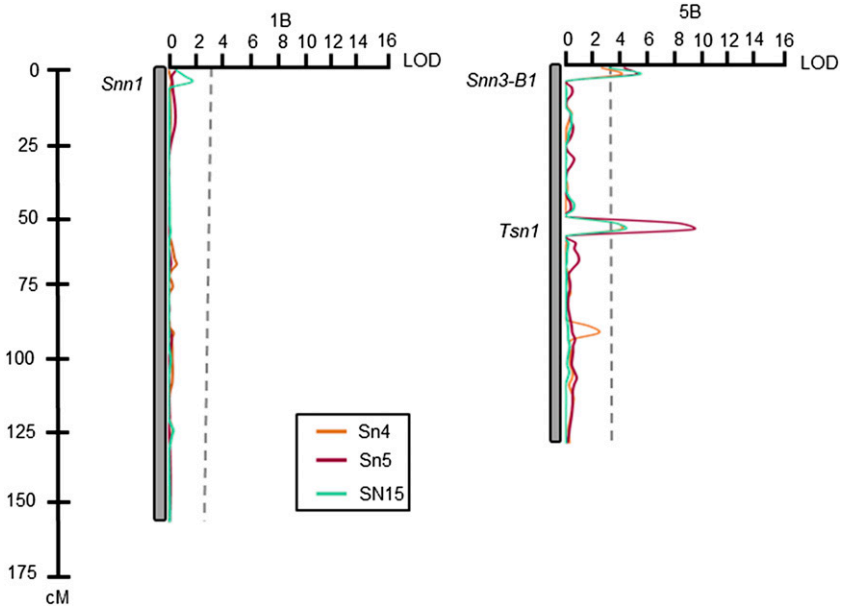

Figure 3. Composite interval regression maps of chromosomes 1B and 5B in the CS-DIC 5B × Sumai 3 recombinant inbred population containing QTL associated with *Parastagonospora nodorum* isolates Sn4, Sn5, and SN15. A cM scale is indicated on the left of the image. The critical LOD threshold is indicated by the dotted lines, and the LOD scale is on the top along the *x* axis.

Table 3. *Composite multiple interval mapping analysis of susceptibility to SNB caused by* P. nodorum *isolates Sn4, Sn5, and SN15 in the CS-DIC 5B × Sumai 3 population*

Gene	Chromosome Arm	Genetic position (cM)	LOD[a]			R^{2b}			Source
			Sn4	Sn5	SN15	Sn4	Sn5	SN15	
Snn1	1BS	1.4	0.31	0.54	1.72	0.002	0.039	0.020	CS-DIC 5B
Snn3-B1	5BS	1.2	4.17	5.27	5.58	0.173	0.204	0.207	Sumai 3
Tsn1	5BL	63.9	4.13	9.59	4.43	0.192	0.324	0.171	Sumai 3

[a]LOD, determined by the execution of 1,000 permutations on marker and phenotypic datasets; cutoff value yielded was 3.25 for detection of significant QTL. [b]R^2 = coefficient of determination.

CIM analysis of the CDS population infected with isolate Sn2000 revealed three loci significantly associated with SNB susceptibility (Fig. 5; Table 5). The locus with the largest effect was *Tsn1*, which had a LOD of 14.18 and explained a total of 32.7% of the disease variation. The locus with the second largest effect was the *Snn1* locus, which had a LOD of 5.42 and explained 7.1% of the disease variation. *QSnb.fcu-4B* was also associated with susceptibility to Sn2000 with a LOD of 4.89, and it explained 10.1% of the disease variation.

Liu et al. (2012) generated an *SnToxA*-knockout strain of Sn2000, designated as Sn2000KO6-1, and it was used to evaluate the CDS population to determine the effects of the *Snn1*-SnTox1 interaction in the absence of a compatible *Tsn1*-SnToxA interaction. CS-DIC 5B and Sumai 3 had average reaction types of 2.10 (moderately resistant) and 0.60 (resistant), respectively (Fig. 4; Tables 1 and 6; Supplemental Fig. S2). The CDS population had an average disease score of 2.02 and a population range of 0.00 to 4.00 (Table 1; Supplemental Fig. S2).

Analysis of the reaction type means of the two genotypic classes revealed that lines containing *Snn1* were significantly more susceptible in their reaction to Sn2000KO6-1 compared with lines without (Table 6), indicating that the *Snn1*-SnTox1 interaction played a significant role in the development of SNB. CIM analysis of the CDS population infected with isolate Sn2000KO6-1 revealed that the *Snn1* locus had a LOD of 12.90 and explained 30.2% of the disease variation (Fig. 5; Table 5). *QSnb.fcu-4B* was also associated with Sn2000KO6-1 susceptibility with a LOD of 15.60 and explained 34.4% of the disease variation.

Expression Analysis of *SnTox1* in Planta using RNA Sequencing

RNA sequencing analysis was conducted to determine whether *SnTox1* expression differed between *P. nodorum* isolates Sn4, Sn5, and SN15. Previous research on *SnTox1* expression has shown that expression is greatest around 48 h and then begins to decline (Liu et al., 2012); therefore, we inoculated the RIL CDS37, which contains all three NE sensitivity genes (*Snn1/Snn3-B1/Tsn1*), and began tissue collection at 48 h post inoculation (hpi). RNA sequencing of *P. nodorum* isolates Sn4, Sn5, and SN15 at in planta postinoculation time points of 48, 72, and 96 hpi yielded an average of 13,005,965 reads per library and ranged from 1,093,752 to 25,560,987 reads (Supplemental Table S4). The majority of reads corresponded to wheat mRNA and, therefore, did not map to the reference genome of isolate LDN03-Sn4. The average percent of reads mapping to the fungal genome ranged from 0.03% to 0.53% with an average of 0.11%. Differential expression analysis revealed that *SnTox1* was significantly up-regulated in isolate SN15 compared with isolates Sn4 and Sn5 at 48 hpi ($P = 0.0031$ and $P = 0.0033$, respectively; Fig. 6). No expression was detected in isolates Sn4 and Sn5 at 48 hpi, whereas SN15 had a normalized read count of 14.06 (Fig. 6). No significant differences in *SnTox1* expression were detected at 72 hpi or 96 hpi between the three isolates. At 72 hpi, SN15, Sn4, and Sn5 had normalized read counts of 3.13, 4.87, and 1.02, respectively. At 96 hpi, SN15, Sn4, and Sn5 had normalized read counts of 1.70, 2.18, and 1.03, respectively. These results indicate *P. nodorum* isolate SN15 expresses *SnTox1* at comparatively higher levels during early in planta time points, but expression then declines over time to levels comparable with those observed in isolates Sn4 and Sn5.

Comparison with all genes encoding predicted secreted proteins, as well as predicted effectors, revealed that *SnTox1* is relatively highly expressed in isolate SN15 at 48 h postinoculation. Out of the total 1239 genes encoding predicted secreted proteins, expression of 305 genes was detected with *SnTox1* being the second highest expressed gene, behind CJJ16_03445, a glycosyl hydrolase. Among all 219 genes encoding predicted effectors, expression of a total of 38 genes was detected

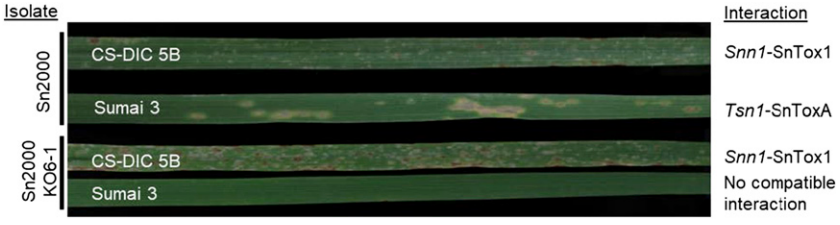

Figure 4. Leaves of CS-DIC 5B and Sumai 3 inoculated with different *Parastagonospora nodorum* isolates. CS-DIC 5B has the NE sensitivity gene *Snn1*, whereas Sumai 3 has *Snn3-B1* and *Tsn1*. *P. nodorum* isolate Sn2000 contains the NE genes *SnTox1* and *SnToxA*, whereas Sn2000KO6 contains the NE gene *SnTox1*.

Table 4. *The different genotypic classes in the CS-DIC 5B × Sumai 3 recombinant inbred population and their average reaction score to the* P. nodorum *isolate Sn2000*

Genotype	No. RIL	Sn2000 Average Reaction Type[a]
CS-DIC 5B	—[b]	2.00 ± 0.60
Sumai 3	—	2.56 ± 0.86
Snn1/Tsn1	23	2.66ab
snn1/tsn1	28	1.12c
Snn1/tsn1	35	2.27b
snn1/Tsn1	32	2.88a
$LSD_{0.05}$	—	0.47

[a]Numbers followed by the same letter in the same column are not significantly different at the 0.05 level of probability. [b]—, Nonapplicable

with *SnTox1* being expressed the highest (Supplemental File S1). These results indicate *P. nodorum* isolate SN15 is expending considerable energy in the expression of *SnTox1* at 48 hpi compared with the rest of the secretome and effectorome.

SnTox1 Expression was Increased in the Absence of *SnToxA*

To investigate whether *SnTox1* expression increases in the *SnToxA*-disrupted strain Sn2000KO6-1 compared with the wild-type isolate Sn2000, or whether the change in QTL magnitude was due to the absence of *SnToxA*, we measured *SnTox1* expression in both Sn2000-and Sn2000KO6-1–infected plants using reverse transcription-quantitative PCR (RT-qPCR). Leaf tissue samples were collected at 12, 24, 48, 72, and 96 hpi for the RIL CDS37, which contains all three genes (*Snn1/Snn3-B1/Tsn1*). *SnToxA* expression was also evaluated and was only expressed in Sn2000 and not Sn2000KO6-1, which lacks *SnToxA* (data not shown). *SnTox1* expression was significantly increased in CDS37 inoculated with Sn2000KO6-1 compared with Sn2000-inoculated plants, except for at the 12 hpi time point (Fig. 7). The highest level of *SnTox1* expression occurred at 72 hpi, where expression was increased 4-fold in plants inoculated with Sn2000KO6-1 compared with the wild-type Sn2000 (Fig. 7).

Promoter Region and Protein Sequence Comparison

The promoter region of *SnTox1* was extracted from the SN15 and Sn4 reference genome sequences (Syme et al., 2016; Richards et al., 2018). Due to the lack of a contiguous genome sequence in Sn5, the *SnTox1* region of that isolate was PCR amplified and sequenced using the Sanger method. The resulting sequence alignment included 915 bp upstream of the start codon and 138 bp of coding sequence. Sequence comparison revealed a 401-bp deletion in the putative promoter region in isolate SN15 located 268 bp upstream of the start codon (Supplemental Fig. S3). Protein alignments revealed that Sn4 and Sn5 harbor identical SnTox1 isoforms, whereas the isoform present in SN15 contained seven amino acid substitutions (Supplemental Fig. S4). These results indicate that extensive polymorphism within the putative regulatory region or between protein isoforms may account for the differences in expression observed for *SnTox1* in isolate SN15.

Although no significant differences in the expression of *SnToxA* and *SnTox3* were observed (Supplemental Fig. S5; Supplemental Fig. S6), their respective putative promoter regions and protein sequences were also compared among the three isolates. A 795-bp region upstream of the start codon of *SnToxA* was aligned between the three isolates, revealing a total of four SNPs and a single base pair deletion (Supplemental Fig. S7). Additionally, a 43-bp insertion was found in isolate SN15, 369 bp upstream of the start codon. The protein sequence of SnToxA was conserved between isolates Sn4 and Sn5; however, the SN15 isoform differed by two amino acids (Supplemental Fig. S8). A higher level of conservation between isolates was observed at the *SnTox3* locus. In the 822 bp upstream of the start codon, isolates Sn4 and Sn5 harbored identical sequences (Supplemental Fig. S9). The same genomic region in isolate SN15 differed only by a single SNP. Additionally, all three isolates share identical protein isoforms (Supplemental Fig. S10).

DISCUSSION

Relative Effects of the Three Compatible Host-NE Interactions

The relationships between biotrophic pathogens and their hosts have been studied extensively with the occurrence of multiple gene-for-gene interactions normally leading to a similar level of resistance as a single interaction. Less research is available on how host

Table 5. *Single-trait multiple interval mapping analysis of susceptibility to SNB caused by* P. nodorum *isolates Sn2000 and Sn2000KO6-1 in the CS-DIC 5B × Sumai 3 population*

Gene	Chromosome arm	Genetic position (cM)	LOD[a]		R^{2b}		Source
			Sn2000	Sn2000KO6	Sn2000	Sn2000KO6	
Snn1	1BS	1.4	5.42	12.90	0.071	0.302	CS-DIC 5B
QSnb.fcu-4B	4BL	55.7	4.86	15.60	0.101	0.344	CS-DIC 5B
Tsn1	5BL	63.9	14.18	—[c]	0.327	—	Sumai 3

[a]LOD, determined by the execution of 1,000 permutations on marker and phenotypic datasets; cutoff value yielded was 3.25 for detection of significant QTL. [b]R^2 = coefficient of determination. [c]—, Nonsignificant.

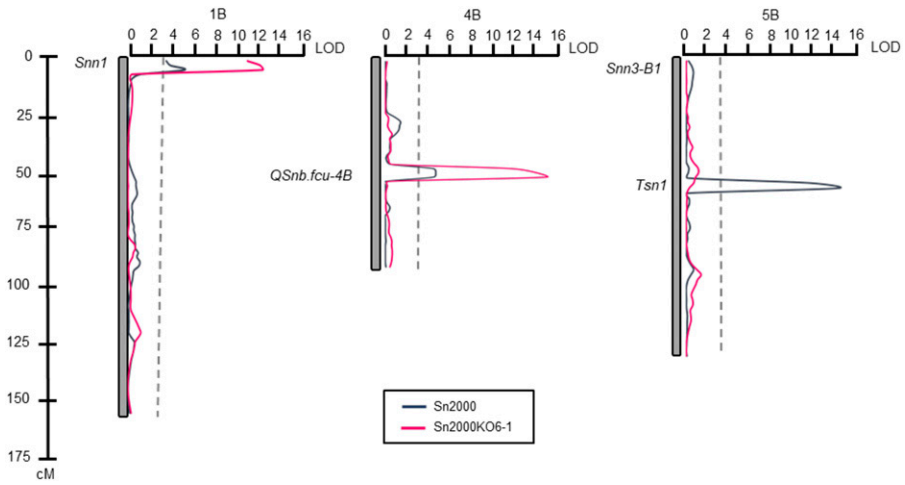

Figure 5. Composite interval regression maps of chromosomes 1B and 5B in the CS-DIC 5B × Sumai 3 recombinant inbred population containing QTL associated with *Parastagonospora nodorum* isolates Sn2000 and Sn2000KO6-1. A cM scale is indicated on the left of the image. The critical LOD threshold is indicated by the dotted lines, and the LOD scale is on the top along the *x* axis.

susceptibility gene-NE interactions differ between isolates in their importance for disease contribution and how different NE genes interact and regulate one another. In this study, we evaluated the relative effects of the *Snn1*-SnTox1, *Snn3-B1*-SnTox3, and *Tsn1*-SnToxA interactions in a single biparental population using multiple fungal isolates/strains. The effects of the three host gene-NE interactions among the three isolates that produced all three NEs were similar in some ways, but there were obvious and interesting dissimilarities as well, which are summarized in Supplemental Table S5. The effects of the *Snn3-B1*-SnTox3 and *Tsn1*-SnToxA interactions were associated with SNB caused by all three isolates. However, the effects of the *Snn1*-SnTox1 were more subtle; therefore, it was investigated in more detail through *SnTox1* expression analysis using RNA sequencing and RT-qPCR.

Snn3-B1-SnTox3 and *Tsn1*-SnToxA

The effects of the *Snn3-B1*-SnTox3 and *Tsn1*-SnToxA interactions were significantly associated with SNB caused by the three isolates that produced all three NEs. However, the effects of these two interactions differed among these isolates. The effects of the *Snn3-B1*-SnTox3 interaction on disease were fairly consistent for the three isolates explaining from 17.3% to 20.7% of the variation, whereas the effects of the *Tsn1*-SnToxA interaction varied much more ranging from 17.1% to 32.4%. Faris et al. (2011) evaluated the effects of the *Tsn1*-SnToxA interaction in SNB development caused by isolates Sn4 and Sn5 in the BR34 × Grandin population and showed that the interaction explained more of the variation in SNB caused by Sn5 than Sn4, which agrees with the results of the current study where *Tsn1*-SnToxA explained 17.9% and 32.4% of the variation for Sn4 and Sn5, respectively.

Other dissimilarities in the relative effects of the *Snn3-B1*-SnTox3 and *Tsn1*-SnToxA interactions among isolates were observed in the genotypic classification analyses. The two interactions contributed equally to disease caused by Sn4 and SN15, and *Tsn1*-SnToxA contributed more to disease caused by Sn5 than did *Snn3-B1*-SnTox3, but only in the absence of the *Snn1*-SnTox1 interaction.

Previous research involving these three isolates in the BR34 × Grandin population showed that the effects of the *Snn2*-SnTox2 and *Tsn1*-SnToxA interactions were additive, and that the *Snn2*-SnTox2 interaction was epistatic to *Snn3-B1*-SnTox3 (Friesen et al., 2007, 2008; Faris et al., 2011). Phan et al. (2016) recently showed in a study using isolate SN15 that *Snn1*-SnTox1 was epistatic to *Snn3-B1*-SnTox3. However, interactions between *Snn3-B1*-SnTox3 and *Tsn1*-SnToxA have not been evaluated. Here, our results showed that the effects of *Snn3-B1*-SnTox3 and *Tsn1*-SnToxA were not additive except for disease caused by SN15 in the absence of a compatible *Snn1*-SnTox1 interaction. Together, these results indicate that host-NE gene interactions are complex and range from additive to epistatic. From our sequencing data of *SnTox3* within each isolate, there are no differences in the promotor and coding region sequences, which correspond to the observed contribution of the *Snn3-B1*-SnTox3 interactions being similar in each isolate. Our initial hypothesis for the difference in *SnToxA* expression and contribution to SNB between isolates Sn4, Sn5, and SN15, with Sn5 having significantly higher expression at 48 hpi and a higher QTL magnitude, was that Sn5 contains a

Table 6. *The different genotypic classes in the CS-DIC 5B × Sumai 3 recombinant inbred population and their average reaction score to the* P. nodorum *isolate Sn2000KO6-1*

Genotype	No. RIL	Sn2000KO6 Average Reaction Type[a]
CS-DIC 5B	—[b]	2.10 ± 0.42
Sumai 3	—	0.60 ± 1.08
Snn1	58	2.51a
snn1	60	1.57b
$LSD_{0.05}$	—	0.36

[a]Numbers followed by the same letter in the same column are not significantly different at the 0.05 level of probability. [b]—, Nonapplicable

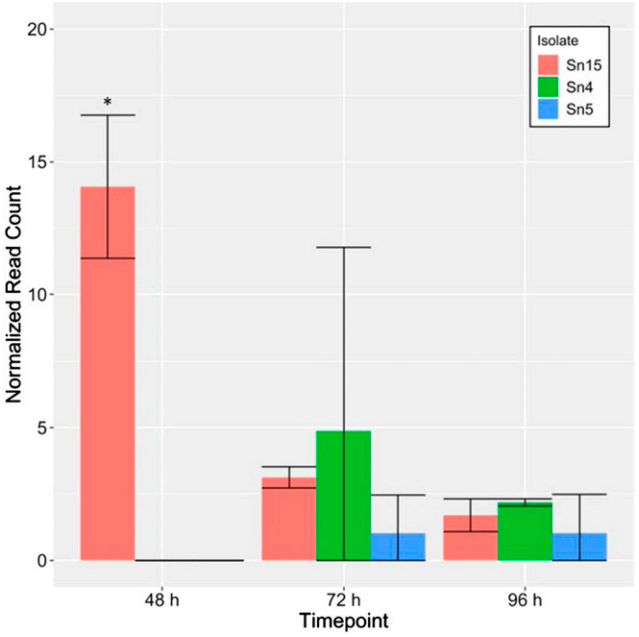

Figure 6. RNA sequencing–evaluated expression of *SnTox1* in the susceptible line CDS37 (*Snn1*/*Snn3-B1*/*Tsn1*) inoculated with *Parastagonospora nodorum* isolates SN15, Sn4, and Sn5 at 48, 72, and 96 h after inoculation. The expression level is shown as the average normalized read count ($n = 2$) from RNA sequencing. SE bars are shown. *Significant differential expression calculated from a Wald test implemented in DESeq2 ($P < 0.01$) compared with other isolates within the same time point.

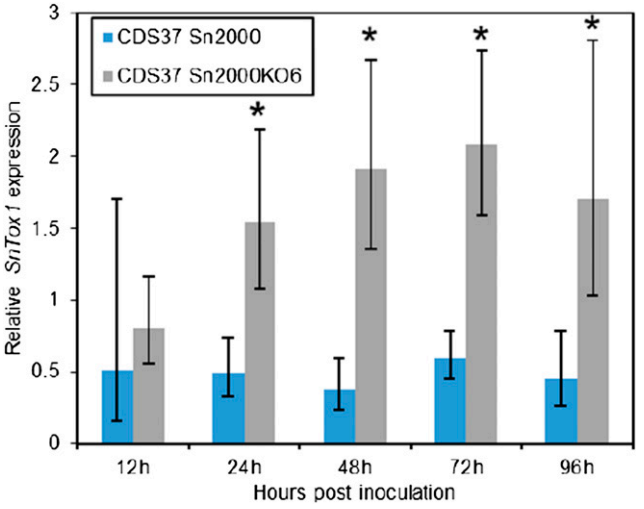

Figure 7. RT-qPCR–evaluated transcriptional expression of *SnTox1* in the susceptible line CDS37 (*Snn1*/*Snn3-B1*/*Tsn1*) inoculated with *Parastagonospora nodorum* isolates Sn2000 and Sn2000KO6-1 at 12, 24, 48, 72, and 96 h after inoculation. The expression of *SnTox1* was normalized to the expression of *Act1*. Average gene expression was calculated from six biological samples in three technical replicates ($n = 6$). SE bars are shown. *Significant differences ($P < 0.05$) between Sn2000 and Sn2000KO6-1 at that time point using a *t* test.

different protein isoform or promotor sequence of *SnToxA* than the other two isolates. However, our sequencing analysis between the three isolates showed no differences in the promotor and amino acid sequences in *SnToxA*, with only very minor differences in the sequences for SN15. The difference in expression and disease contribution from the *Tsn1*-SnToxA interaction when plants are infected with Sn5 may be due to transposable elements and other genetic factors near *SnToxA*, which will be discussed below. However, no full genome sequence of Sn5 exists. Additionally, other host-pathogen interactions may be involved in regulating virulence dictated by host sensitivity gene-NE interactions.

Snn1-SnTox1

The *Snn1*-SnTox1 interaction did not contribute to SNB caused by Sn4 or Sn5, and in SN15, it contributed to disease only in the absence of compatible *Snn3-B1*-SnTox3 and *Tsn1*-SnToxA interactions indicating that the latter two are epistatic to *Snn1*-SnTox1. This is contrary to the findings of Phan et al. (2016) who, using the same isolate, reported that the *Snn1*-SnTox1 interaction was epistatic to *Snn3-B1*-SnTox3. A possible explanation for the differences between the two studies is likely the presence of different host alleles at the *Snn1* and/or *Snn3-B1* loci, with Sumai 3 containing an allele associated with a stronger reaction to a compatible *Snn3-B1*-SnTox3 interaction (Shi et al., 2016a) than the *Snn3-B1* donor parent in Phan et al. (2016).

Not only did the *Snn1*-SnTox1 interaction contribute little to susceptibility, some evidence suggested that the involvement of the *Snn3-B1*-SnTox3 and *Tsn1*-SnToxA interactions in disease was reduced in the presence of *Snn1*-SnTox1. For example, the *Tsn1*-SnToxA interaction contributed more than *Snn3-B1*-SnTox3 to SNB caused by Sn5, but only in the absence of *Snn1*-SnTox1. Also observed in the Sn5 analysis, the presence of *Snn3-B1*-SnTox3 and *Tsn1*-SnToxA led to more disease than when all three interactions were present, indicating that a compatible *Snn1*-SnTox1 interaction actually reduced disease under that scenario. Also, the finding that *Snn3-B1*-SnTox3 and *Tsn1*-SnToxA were additive only in the absence of *Snn1*-SnTox1 in SNB caused by SN15 would suggest further that a compatible *Snn1*-SnTox1 may inhibit disease when in the presence of some other interactions.

Another reason for the discrepancy between the Phan et al. (2016) study and ours may pertain to the nontypical phenotype of the compatible *Snn1*-SnTox1 interaction. The *Snn1*-SnTox1 interaction is unique in that it not only produces lesions, but also necrotic flecks that sometimes, but not always, lead to larger lesions (Liu et al., 2004b, 2012, 2016; Shi et al., 2016b). The flecks do not fit the descriptions of lesions in the 0–5 lesion type rating scale used in this study and are therefore largely unaccounted for even though they undoubtedly lead to a decrease in the photosynthetic material on the leaf.

Perhaps digital imaging of infected leaves or similar methods would lead to more accurate scores and hence the association of the *Snn1*-SnTox1 interaction with the development of SNB. It is interesting to note that Xu et al. (2004) found a significant correlation between SNB resistance and the flecking caused by the *Snn1*-SnTox1 interaction in synthetic hexaploid wheat lines. This would lend support to our findings noted above that *Snn1*-SnTox1 may sometimes contribute to resistance. However, it has been clearly demonstrated that SnTox1 is an NE that, when recognized by the *Snn1* gene product, leads to host responses that result in NETS in an inverse gene-for-gene fashion (Liu et al., 2004a, 2012, 2016; Chu et al., 2010; Shi et al., 2016b). It may be that the putative PTI pathway activated by a compatible *Snn1*-SnTox1 interaction may antagonize or inhibit the response of the ETI pathways activated by other interactions such as *Snn3-B1*-SnTox3 and *Tsn1*-SnToxA. More work is needed to decipher the molecular interplay of these interactions.

SnTox1 Is Differentially Expressed between Isolates as Shown using RNA Sequencing

To examine whether the *Snn1*-SnTox1 interaction was being masked by the other interactions or whether *SnTox1* was expressed at lower levels in Sn4 and Sn5 compared with SN15, we performed an RNA sequencing experiment. The data from RNA sequencing indicate that when comparing the three isolates, *SnTox1* expression was highest in SN15 at 48 hpi but was not significantly different between the three isolates at 72 and 96 hpi. This corroborates our genetic analyses where the *Snn1/snn3-B1/tsn1* lines had significantly more disease than *snn1/snn3-B1/tsn1* lines. These findings indicate that the level of disease contributed by a compatible *Snn1*-SnTox1 interaction varies among these three isolates and is likely due to differences in *SnTox1* expression in the pathogen and not host differences. Previously, it was shown that SnTox1 acts as a dual-function protein and protects the fungus from wheat chitinases during the infection process (Liu et al., 2016). Isolates that contain *SnTox1* may express this NE at low levels for protection; however, the pathogen may down-regulate *SnTox1* to prevent it from playing an important role in eliciting a host response. This may be occurring in *P. nodorum* isolates Sn4 and Sn5. However, we observed that *SnTox1* expression was higher in SN15 along with the *Snn1*-SnTox1 interaction contributing significantly to disease. Our analysis of the SN15 secretome and effectorome showed that *SnTox1* is highly expressed among all secreted proteins and is the highest expressed effector at 48 hpi. Some isolates, such as SN15, may express *SnTox1* at high levels so the SnTox1 protein can provide both protection along with eliciting disease, whereas other isolates may use other NE for eliciting disease. Potentially, pathogens may have the ability to 'determine' which host sensitivity genes are present through feedback mechanisms and increase the expression of the corresponding NE genes to maximize disease while balancing the cost of expression. One explanation for the differences in *SnTox1* expression between isolates may be epigenetic regulation. Recently, Haueisen et al. (2019) examined the expression profiles after infection of three isolates of *Zymoseptoria tritici*, a hemibiotrophic wheat pathogen. Many of the differentially expressed genes between the isolates were effector candidate genes and were located within 2 kb of transposable elements. Located next to *SnTox1* is a short truncated molly-type retrotransposable element (Liu et al., 2012). Whether epigenetic transcriptional regulation of the transposable element close to *SnTox1* plays a role in influencing *SnTox1* expression would need to be further studied to validate or disprove if this type of regulation network is also occurring in *P. nodorum*. Another potential mechanism governing the differences in *SnTox1* expression may be transcription factors (TFs), which are further discussed below.

Differences in NE Gene Promoter and Protein Sequences May Influence the Importance of Different Sensitive Gene-NE Interactions in Causing Disease and Variation between Isolates

Amino acid and promoter sequence alignments for *SnTox1* revealed multiple polymorphisms in SN15 compared with Sn4 and Sn5, with the latter two being nearly identical. The 401-bp deletion in the promotor region of the SN15 *SnTox1* gene might be important for transcription factor binding, with the deleted sequence promoting higher *SnTox1* expression. Additionally, the SnTox1 protein isoform differed between SN15 compared with Sn4 and Sn5, with seven amino acid changes between them. These changes could influence SnTox1 protein binding with the Snn1 protein, with the SN15 isoform having a higher binding affinity. Further studies are needed to test these hypotheses, along with identifying transcription factors and other regulators of *SnTox1*.

Effects of the Inverse Gene-For-Gene Interactions using the NE Gene-Disrupted Mutant Isolates

Infection of the CDS population with isolate Sn2000, which does not have *SnTox3*, indicated that both the *Snn1*-SnTox1 and *Tsn1*-SnToxA interactions were associated with SNB susceptibility. This agreed with the findings of Chu et al. (2010) who used the same isolate on a different wheat population. However, Chu et al. (2010) showed that the effects of the two interactions were largely additive, whereas they were not additive in the CDS population. Chu et al. (2010) also inoculated their population with the *SnToxA*-knockout isolate Sn2000KO6-1 and found that the effects of the *Snn1*-SnTox1 interaction increased from explaining 22% of the variation in the wild-type isolate to 50% in the

SnToxA-knockout isolate. Their findings agree with the results of this research where the *Snn1*-SnTox1 interaction went from explaining 7.1% of the variation in Sn2000 to 30.2% in the *SnToxA*-knockout isolate. The increase in necrotic flecking and disease in *Snn1* plants infected with Sn2000KO6-1 compared with the wild type was a result of increased levels of *SnTox1* transcription, which agrees with previous findings that NE gene transcriptional expression levels dictate the levels of NETS that occur in wheat-*P. nodorum* inverse gene-for-gene interactions (Faris et al., 2011; Phan et al., 2016; Virdi et al., 2016).

We demonstrated that when *SnToxA* is eliminated from Sn2000, the expression of *SnTox1* is significantly increased. Manning and Ciuffetti (2015) reported that *ToxA* is epistatic to other effector genes in *P. tritici-repentis*. Further research is needed to determine whether *SnToxA* is truly epistatic to *SnTox1* or if other mechanisms in the pathogen are leading to changes in *SnTox1* expression in the absence of *SnToxA*.

Previous research has suggested that *SnTox1* is epistatic to *SnTox3* (Phan et al., 2016). Further studies are needed to determine whether this was an isolate-specific case or if this is true for all *P. nodorum* isolates that contain *SnTox1* and *SnTox3*, because the opposite was observed in this study. Recently published literature has reported that multiple transcription factors are responsible for NE gene regulation. The C2H2 zinc finger transcription factors *P. nodorumCon7* (*PnCon7*), a zinc finger transcription factor, and *Stagonospora nodorum StuA*, an ASM-1, Phd1, StuA, EFG1, and Sok2 domain transcription factor, have been reported to be regulators of *SnTox3* (IpCho et al., 2010; Lin et al., 2018). Lin et al. (2018) found through silencing of *PnCon7*, there was a corresponding decrease in *SnTox3* expression. Although PnCon7 was found to not be directly correlated with *SnTox1* expression, silencing of *PnCon7* led to decreased *SnTox1* and *SnToxA* expression. Additionally, the zinc finger transcription factor PnPf2 is a conserved signaling component that regulates both *SnToxA* and *SnTox3* expression (Rybak et al., 2017).

It might be possible that some TFs regulate multiple NE genes, or that there are global regulators of NE genes. When one NE gene is eliminated from an isolate, there would be up-regulation of the other NE genes due to fewer promoter sites competing for TF binding. To test this hypothesis, expression levels for multiple NE genes in multiple isolates would need to be determined and compared with knockout strains of different combinations of NE genes. Additionally, no common TF that binds to a conserved promoter region in *SnTox1*, *SnTox3*, and *SnToxA* has yet been identified. As stated, whether NE genes are truly regulating one another (i.e. are epistatic to one another) or if they are controlled by global regulators has yet to be determined. Findings from this study along with previously published research suggest that regulation within *P. nodorum* for NE genes is complex and that we are just beginning to unravel this conundrum.

CONCLUSION

Overall, the results of this study show that all three host sensitivity gene-NE interactions can contribute to the development of SNB. However, their relative effects on disease expression varied from additive to epistatic, and in no case did all three compatible interactions simultaneously contribute significantly to disease development. This observation, along with the results obtained from evaluating the NE gene-knockout mutant isolate and NE gene expression, suggests that the pathogen likely has a target threshold for NE production. It is possible that, although the fungus may harbor numerous NE genes, which ones are expressed and to what levels may depend on the repertoire of NE sensitivity genes present in the host under attack. If the pathogen 'determines' that the host harbors multiple NE sensitivity genes that it can exploit because it harbors the corresponding NE genes, then perhaps the pathogen strives to find a balance between the amount of energy it needs to expend to express NE genes and what it needs to do to propagate and complete its lifecycle. In other words, it is probably not efficient for the pathogen to always produce numerous NEs if it can achieve infection and sporulation by producing one or two. Clearly, these host-pathogen interactions are complex and can be affected by multiple factors, and more work related to the interplay between interactions, pathogen NE genes, and host sensitivity genes is required.

From a more applied perspective, the results of this research reiterate the importance of *Snn1*, *Tsn1*, and *Snn3-B1* in conferring SNB susceptibility in wheat. We therefore continue to recommend that breeders remove the dominant susceptibility alleles from their materials, which can be done efficiently using molecular markers (Faris et al., 2010; Shi et al., 2016a, 2016b). Additionally, recent research (Gao et al., 2015; Phan et al., 2016; Rybak et al., 2017) along with the findings from this study are beginning to unravel the role NE gene expression plays in SNB development and severity along with the complex regulatory mechanisms of these NE genes.

MATERIALS AND METHODS

The RIL Mapping Population

An RIL population composed of 190 lines was developed from a cross between the hexaploid *Triticum aestivum* (wheat) line Sumai 3 and the Chinese Spring-*Triticum turgidum* ssp. *dicoccoides* chromosome 5B disomic substitution line (CS-DIC 5B), which are both landraces from China. Sumai 3 contains the *Tsn1* and *Snn3-B1* genes, which confer sensitivity to SnToxA and SnTox3, respectively, and CS-DIC 5B has the *Snn1* gene and is therefore sensitive to SnTox1. *Tsn1* was previously cloned by Faris et al. (2010) and is a present/absent variant that is present in Sumai 3 and null in CS-DIC 5B. *Snn1* was previously cloned by Shi et al. (2016b), with Sumai 3 having the recessive allele and CS-DIC 5B having the dominant allele. *Snn3-B1* has yet to be cloned. The RILs were developed using the single-seed descent method and were bulked at the F_7 generation with the population designated as CDS.

Infiltrations

The *Parastagonospora nodorum* genes *SnTox1*, *SnToxA*, and *SnTox3* have previously been cloned and expressed in *Pichia pastoris* to produce

NE-containing culture filtrates (Friesen et al., 2006; Liu et al., 2009, 2012). SnTox1, SnTox3, and SnToxA were obtained from *Pichia pastoris* cultures producing these NEs as described by Liu et al. (2009).

Plants were grown, infiltrated, and evaluated 5 d after infiltration as described in Zhang et al. (2011). Reaction types of 2 and 3 were considered sensitive, and 0 and 1 were insensitive. The experiment was performed twice and analyzed using a χ^2 analysis.

SSR and SNP Analysis

DNA was extracted from leaf tissue as described by Faris et al. (2000) and diluted to ~200 ng/μL using distilled water. An SSR primer survey using parental DNA (CS-DIC 5B and Sumai3) was used to identify markers that reveal polymorphism between the parents. Markers for the survey were chosen based on previously published locations, which were obtained from the GrainGenes database (http://wheat.pw.usda.gov/GG2/index.shtml). SSR markers located on chromosome arms 1BS, 5BL, and 5BS, within the known vicinity of the *Snn1*, *Tsn1*, and *Snn3-B1* genes, respectively (Faris et al., 1996; Liu et al., 2004b; Friesen et al., 2008), were considered the highest priority. Three to six additional SSR markers that detect loci on the other wheat chromosomes were selected to assist with assigning linkage groups to chromosomes. The polymorphic SSR markers were selected from the following libraries: WMC (Somers et al., 2004), WMS (marker designation = 'gwm'; Röder et al., 1998), MAG (Xue et al., 2008), HBG (Torada et al., 2006), CFD (Sourdille et al., 2004), BARC (Song et al., 2005), GDM (Pestsova et al., 2000), HBE (Torada et al., 2006), HBD (Torada et al., 2006), PSP (Bryan et al., 1997), FCP (Reddy et al., 2008; Shi et al., 2015), CFA (Sourdille et al., 2004), and CFB (Sourdille et al., 2004).

DNA fragments were amplified using PCR and the markers chosen above. PCR reactions consisted of 200 ng of template DNA, 1× PCR buffer, 2 mM $MgCl_2$, 0.2 mM deoxynucleotide triphosphates, 4 pmol of each primer, and 0.5 unit of *Taq* DNA polymerase, with diluted water added to a final volume of 10 μL. PCR was performed using a GeneAmp PCR system 9700 machine. The PCR cycle was as follows: 94°C for 5 min, cycle 35 times through: 30 s 94°C, 30 s 65–56°C, 90 s 72°C; finishing with one cycle for 7 min at 72°C and cooling to 4°C. PCR products were separated on 6% polyacrylamide gels, stained with GelRed nucleic acid gel stain, and scanned on a Typhoon FLA 9500 variable mode laser scanner (GE Healthcare Life Sciences).

The CDS population was also genotyped using a 9K iSelect Assay BeadChip (Cavanagh et al., 2013). A BeadStation and iScan instrument from Illumina were used for the assay. Clustering data were analyzed using GenomeStudio Polyploid Clustering Module from Illumina, Inc. (2013).

The SSR marker, NE infiltration, and SNP data were combined to develop genetic linkage maps of all 21 chromosomes. The computer software MapDisto version 1.7 (Lorieux, 2012) was used to assemble the linkage maps as described in Faris et al. (2014). The Kosambi mapping function was used to calculate the map distances (Kosambi, 1944).

Inoculations with *P. nodorum* Isolates

Methods for plant inoculation were as described by Friesen and Faris (2012). Conidia of *P. nodorum* isolates LDN03Sn4 (Sn4), BBC03Sn5 (Sn5), Sn2000, Sn2000KO6-1, and AuSN15 (SN15) were used to phenotype the population. Sn4, Sn5, and SN15 were previously found to contain *SnToxA*, *SnTox1*, and *SnTox3* (Friesen et al., 2007; Hane et al., 2007; Faris et al., 2011; Gao et al., 2015; T.L. Friesen, unpublished data). Sn2000 contains *SnToxA* and *SnTox1* (Liu et al., 2004b), and Sn2000KO6-1 contains *SnTox1* (Liu et al., 2012; Supplemental Table S6).

Three plants per line were grown in plastic cones that were 3.8 cm in diameter and 21 cm deep (Stuewe and Sons, Inc.). A total of 118 RILs and the parental lines were inoculated in a completely randomized design. The susceptible wheat cultivar Alsen was grown on the outside borders of the racks to reduce any edge effect. Plants were inoculated following the methods in Friesen et al. (2007). Plants were scored at 7 d after inoculation using a 0 to 5 scoring scale described by Liu et al. (2004a) where 0 = highly resistant and 5 = highly susceptible.

Inoculations of each isolate were replicated at least three times with randomization between replicates (Supplemental Table S3). The homogeneity of variances among the replicates was determined by Barlett's χ^2 test using the general linear model procedure in SAS (SAS Institute, 2011). The mean separation of the phenotypic means was determined using Fischer's protected Least Significant Difference (LSD) at an alpha level of 0.05. Phenotypic scores from each replicate were combined to calculate an overall mean if the error of variance was homogenous between replicates.

QTL Analysis

QTL analysis was conducted using the computer software program QGene v 4.3.10 (Joehanes and Nelson, 2008). Composite interval mapping was used to quantify the effects of the *Tsn1*, *Snn1*, and *Snn3-B1* loci in conferring susceptibility to the various isolates, and also to identify putative novel QTLs associated with resistance. The coefficient of determination (R^2) was used to indicate the amount of variation explained by the QTLs and therefore provide an estimate of the contribution of each compatible host-NE interaction in the development of SNB. Critical LOD thresholds at the 0.05 and 0.01 levels of probability were determined using a permutation test with 1000 iterations.

RNA Sequencing

Plants of the RIL CDS37, which has the genotype *Snn1*/*Snn3-B1*/*Tsn1*, were grown and inoculated with Sn4, Sn5, SN15, Sn2000, and Sn2000KO6-1 as described above. Leaf tissue samples for each genotype and isolate combination were collected from the second leaf at 48, 72, and 96 h after inoculation and immediately frozen in liquid nitrogen and stored at −80° until mRNA extraction. Tissue from three samples for each isolate was pooled to make one technical replicate, with a total of two technical replicates used. mRNA was isolated using the Dynabeads mRNA Direct Kit (Life Technologies) following the manufacturer's protocol. With use of purified mRNA as the input, strand nonspecific RNAseq libraries were prepared with the Illumina TruSeq RNA Sample Preparation v2 following the manufacturer's recommended protocol. Fragment size distribution of the prepared RNAseq libraries was determined using an Agilent DNA chip on a bioanalyzer (Agilent). Quality and concentrations were determined using KAPA Library Quantification Kit (Roche Molecular Systems) following the Illumina platforms portion of the protocol, and qPCR was run on a Roche LightCycler 480 II. Libraries were sequenced on an Illumina NextSeq 500 at the U.S. Department of Agriculture (USDA)-Agricultural Research Service Small Grains Genotyping Center to produce 150-bp single-end reads.

Bioinformatics and Differential Expression Analysis

Sequencing reads were examined for quality metrics using FastQC (Andrews, 2010). Reads were quality trimmed using trimmomatic (Bolger et al., 2014) to remove adaptor sequences, trim based on quality via a sliding window, remove the leading 10 nucleotides, and discard reads less than 36 bp (ILLUMINACLIP:illumina_sequences_trimming:2:30:10 SLIDINGWINDOW:4:15 HEADCROP:10 MINLEN:36). Quality trimmed RNA sequencing reads were mapped to the LDN03-Sn4 reference genome (Richards et al., 2018) using HISAT2 (Kim et al., 2015; Pertea et al., 2016) specifying a maximum intron length of 3000 bp. Sequence alignment map files were converted to binary alignment map files and subsequently sorted and indexed using SAMtools (Li et al., 2009). Transcripts were assembled using StringTie under default settings (Pertea et al., 2016). Differential gene expression analysis was conducted using the R package DESeq2, specifically comparing the expression of *SnTox1* in each isolate at each time point (Love et al., 2014). Expression values were calculated as normalized read counts and used for comparison between isolates and time points. Normalized read counts from the DESeq2 analysis were also extracted for genes encoding predicted secreted proteins (secretome), as well as all genes encoding predicted effectors (effectorome), to determine relative expression of *SnTox1* compared with all predicted secreted proteins and effectors at time points with significant differences in expression (J.K. Richards and T.L. Friesen, unpublished data).

De Novo Genome Assembly and Protein Alignments

Illumina short-read sequence of isolate Sn5 was obtained from a related project (J.K. Richards and T.L. Friesen, unpublished data). Sequencing reads were de novo assembled using SPAdes under default settings (Bankevich et al., 2012). Assembled contigs were then used to create a local BLAST database, from which, *ToxA*, *Tox1*, and *Tox3* sequences were identified via 'blastn' (Camacho et al., 2009). In cases where de novo assembled contigs did not contain a complete and contiguous gene sequence, the gene was PCR amplified and sequenced using the Sanger method to provide complete CDS information (Supplemental Table S7). Protein sequences were aligned in Geneious v11.1.5.

For the analysis of polymorphisms within the putative promoter regions, 1000 bp of sequence upstream of the start codons of *SnToxA*, *SnTox1*, and *SnTox3*

was retrieved from the SN15 and Sn4 reference genomes (Syme et al., 2016; Richards et al., 2018) using 'pyfaidx' (Shirley et al., 2015). Because no complete genome sequence of isolate Sn5 was available, primers were designed to amplify the putative promoter regions (Supplemental Table S7), and amplicons were sequenced using the Sanger method.

Transcriptional Expression Analysis using RT-qPCR

Plants of the RIL CDS37, which was sensitive to all three NEs because it has the genotype *Snn1/Snn3-B1/Tsn1*, were grown and inoculated with Sn2000 and Sn2000KO6-1 as described above. Leaf tissue samples for each genotype and isolate combination were collected from the second leaf at 12, 24, 48, 72, and 96 h after inoculation and immediately frozen in liquid nitrogen. RNA extraction and RT-qPCR methods were the same as in Virdi et al. (2016) with the exception of the 10 μL PCR reaction, which contained 1 × SYBR PCR Master Mix (Applied Biosystems), 0.25 μM each primer, and 4 μL of 4-fold diluted complementary DNA. Each experiment was conducted using at least six biological replicates, each consisting of a single inoculated leaf, and at least three technical replicates per biological replicate were performed. Primers for *SnToxA* were ToxA.RT.F3 (5′-AACGCCAATACAGTGCGAGT-3′) and Tox.cod.1R (5′-GCTGCATTCTCCAATTTTCACG-3′), for *SnTox1* were SnTox1RT1F (5′-CTCACGTTTGAGGGCTTAGG-3′) and SnTox1RT1R (5′-GGATGCAATAGAGCAGCAGA-3′), and for the *P. nodorum* actin gene were ActinqPCRf (5′-AGTCGAAGCGTGGTATCCT-3′) and ActinqPCRr (5′-ACTTGGGGTTGATGGGAG-3′). The expression level of the CDS37 sample at 12 h inoculated with Sn2000 was set at 1 as a calibration point. Threshold cycles of the *SnToxA*, *SnTox1*, and endogenous actin gene were used to calculate the relative expression levels using the $2^{-\Delta\Delta CT}$ method. Statistical analysis was performed between each isolate for each line and time point using *t*-test to determine whether significantly different at $P < 0.05$.

Accession Numbers

Sequence data from this article can be found in the GenBank/EMBL data libraries under accession numbers GU259637 for *Tsn1*in Sumai3, KP085710 for *Snn1* in Chinese Spring, and HM191250, MK612041, and MK612040 for *SnToxA*, *SnTox1*, and *SnTox3*, respectively, in Sn5. Whole genome sequences including the NE genes used in this study are present in the National Center for Biotechnology Information database BioProject PRJNA398070 for isolates Sn4 and Sn2000, and BioProject PRJNA13754 for isolate SN15.

Supplemental Data

The following supplemental materials are available:

Supplemental Figure S1. Histograms of the average lesion-type reactions of the CS-DIC 5B × Sumai 3 recombinant inbred population to various *Parastagonospora nodorum* isolates.

Supplemental Figure S2. Histograms of the average lesion-type reaction of the CS-DIC 5B × Sumai 3 recombinant inbred population to *Parastagonospora nodorum* isolates Sn2000 and Sn2000KO6.

Supplemental Figure S3. Alignment of the putative *SnTox1* promoter region in *Parastagonospora nodorum* isolates Sn5, SN15, and Sn4.

Supplemental Figure S4. The amino acid sequence of *SnTox1* in *Parastagonospora nodorum* isolates Sn4, Sn5, and SN15.

Supplemental Figure S5. Expression of *SnToxA* in the susceptible line CDS37 (*Snn1/Snn3-B1/Tsn1*) inoculated with *Parastagonospora nodorum* isolates Sn4, Sn5, and SN15 at 48, 72, and 96 h post inoculation.

Supplemental Figure S6. Expression of *SnTox3* in the susceptible line CDS37 (*Snn1/Snn3-B1/Tsn1*) inoculated with *Parastagonospora nodorum* isolates Sn4, Sn5, and SN15 at 48, 72, and 96 h post inoculation.

Supplemental Figure S7. Alignment of the putative SnToxA promoter region in *Parastagonospora nodorum* isolates Sn5, SN15, and Sn4.

Supplemental Figure S8. The amino acid sequence of SnToxA in *Parastagonospora nodorum* isolates Sn4, Sn5, and SN15.

Supplemental Figure S9. Alignment of the putative SnTox3 promoter region in *Parastagonospora nodorum* isolates Sn5, SN15, and Sn4.

Supplemental Figure S10. The amino acid sequence of SnTox3 in *Parastagonospora nodorum* isolates Sn4, Sn5, and SN15.

Supplemental Table S1. Summary of the genetic linkage maps for each chromosome/genome in the CS-DIC 5B × Sumai 3 population.

Supplemental Table S2. χ^2 analysis for sensitivity to the purified NEs SnTox1, SnTox3, and SnToxA, which interact with the wheat sensitivity genes *Snn1*, *Snn3-B1*, and *Tsn1*, respectively, in the CDS population.

Supplemental Table S3. Bartlett's χ^2 analysis for homogeneity amount replicates used in this study.

Supplemental Table S4. RNA sequencing results for the *P. nodorum* isolates Sn4, Sn5, and SN15 at *in planta* time points 48, 72, and 96 h post infection.

Supplemental Table S5. Summary of the observed interactions in this study for *P. nodorum* isolates Sn4, Sn5, Sn6, SN15, Sn2000, and Sn2000KO6-1 inoculated onto the CS-DIC 5B × Sumai 3 RI population.

Supplemental Table S6. *Parastagonospora nodorum* isolates used in this study along with origin and source of the NE each isolate contains.

Supplemental Table S7. Primers used in this study for sequencing necrotrophic effector genes.

Supplemental File S1. Effectorome and secretome of *P. nodorum* isolate SN15 at 48, 72, and 96 h post inoculation.

ACKNOWLEDGMENTS

The authors thank Samantha Steckler, Danielle Holmes, Jason Axtman, Nathan Wyatt, and Megan Overlander for technical assistance. Mention of trade names or commercial products in this article is solely to provide specific information and does not imply recommendation or endorsement by the USDA. USDA is an equal opportunity provider and employer.

Received February 5, 2019; accepted February 24, 2019; published March 11, 2019.

LITERATURE CITED

Abeysekara NS, Friesen TL, Keller B, Faris JD (2009) Identification and characterization of a novel host-toxin interaction in the wheat-*Stagonospora nodorum* pathosystem. Theor Appl Genet **120:** 117–126

Abeysekara NS, Faris JD, Chao S, McClean PE, Friesen TL (2012) Whole-genome QTL analysis of Stagonospora nodorum blotch resistance and validation of the SnTox4-*Snn4* interaction in hexaploid wheat. Phytopathology **102:** 94–104

Andrews S (2010) FastQC: A quality control tool for high throughput sequence data. http://www.bioinformatics.babraham.ac.uk/projects/fastqc

Bankevich A, Nurk S, Antipov D, Gurevich AA, Dvorkin M, Kulikov AS, Lesin VM, Nikolenko SI, Pham S, Prjibelski AD, et al (2012) SPAdes: A new genome assembly algorithm and its applications to single-cell sequencing. J Comput Biol **19:** 455–477

Bolger AM, Lohse M, Usadel B (2014) Trimmomatic: A flexible trimmer for Illumina sequence data. Bioinformatics **30:** 2114–2120

Bryan GJ, Collins AJ, Stephenson P, Orry A, Smith JB, Gale MD (1997) Isolation and characterization of microsatellites from hexaploid bread wheat. Theor Appl Genet **94:** 557–563

Camacho C, Coulouris G, Avagyan V, Ma N, Papadopoulos J, Bealer K, Madden TL (2009) BLAST+: Architecture and applications. BMC Bioinformatics **10:** 421

Cavanagh CR, Chao S, Wang S, Huang BE, Stephen S, Kiani S, Forrest K, Saintenac C, Brown-Guedira GL, Akhunova A, et al (2013) Genome-wide comparative diversity uncovers multiple targets of selection for improvement in hexaploid wheat landraces and cultivars. Proc Natl Acad Sci USA **110:** 8057–8062

Chu CG, Faris JD, Xu SS, Friesen TL (2010) Genetic analysis of disease susceptibility contributed by the compatible *Tsn1*-SnToxA and *Snn1*-SnTox1 interactions in the wheat-*Stagonospora nodorum* pathosystem. Theor Appl Genet **120:** 1451–1459

Day B, Henty JL, Porter KJ, Staiger CJ (2011) The pathogen-actin connection: A platform for defense signaling in plants. Ann Rev Phytopathol **49:** 483–506

Eyal Z, Scharen AL, Prescott JM, van Ginkel M (1987) The Septoria diseases of wheat: Concepts and methods of disease management. CIMMYT, Mexico

Faris JD, Friesen TL (2009) Reevaluation of a tetraploid wheat population indicates that the *Tsn1*-ToxA interaction is the only factor governing *Stagonospora nodorum* blotch susceptibility. Phytopathology **99:** 906–912

Faris JD, Anderson JA, Francl LJ, Jordahl JG (1996) Chromosomal location of a gene conditioning insensitivity in wheat to a necrosis-inducing culture filtrate from *Pyrenophora tritici-repentis*. Phytopathology **86:** 459–463

Faris JD, Haen KM, Gill BS (2000) Saturation mapping of a gene-rich recombination hot spot region in wheat. Genetics **154:** 823–835

Faris JD, Zhang Z, Lu H, Lu S, Reddy L, Cloutier S, Fellers JP, Meinhardt SW, Rasmussen JB, Xu SS, et al (2010) A unique wheat disease resistance-like gene governs effector-triggered susceptibility to necrotrophic pathogens. Proc Natl Acad Sci USA **107:** 13544–13549

Faris JD, Zhang Z, Rasmussen JB, Friesen TL (2011) Variable expression of the *Stagonospora nodorum* effector SnToxA among isolates is correlated with levels of disease in wheat. Mol Plant Microbe Interact **24:** 1419–1426

Faris JD, Zhang Q, Chao S, Zhang Z, Xu SS (2014) Analysis of agronomic and domestication traits in a durum × cultivated emmer wheat population using a high-density single nucleotide polymorphism-based linkage map. Theor Appl Genet **127:** 2333–2348

Flor HH (1956) Complementary genetic systems in flax and flax rust. Adv Genet **8:** 29–54

Friesen TL, Faris JD (2010) Characterization of the wheat-*Stagonospora nodorum* system: What is the molecular basis of this quantitative necrotrophic disease interaction? Can J Plant Pathol **32:** 20–28

Friesen TL, Faris JD (2012) Characterization of plant-fungal interactions involving necrotrophic effector-producing plant pathogens. *In* MD Bolton and B Thomma,, eds, Plant Fungal Pathogens. Methods in Molecular Biology (Methods and Protocols). Humana Press, Hatfield, United Kingdom, pp 191–207

Friesen TL, Stukenbrock EH, Liu Z, Meinhardt S, Ling H, Faris JD, Rasmussen JB, Solomon PS, McDonald BA, Oliver RP (2006) Emergence of a new disease as a result of interspecific virulence gene transfer. Nat Genet **38:** 953–956

Friesen TL, Meinhardt SW, Faris JD (2007) The *Stagonospora nodorum*-wheat pathosystem involves multiple proteinaceous host-selective toxins and corresponding host sensitivity genes that interact in an inverse gene-for-gene manner. Plant J **51:** 681–692

Friesen TL, Zhang Z, Solomon PS, Oliver RP, Faris JD (2008) Characterization of the interaction of a novel *Stagonospora nodorum* host-selective toxin with a wheat susceptibility gene. Plant Physiol **146:** 682–693

Friesen TL, Chu CG, Liu ZH, Xu SS, Halley S, Faris JD (2009) Host-selective toxins produced by *Stagonospora nodorum* confer disease susceptibility in adult wheat plants under field conditions. Theor Appl Genet **118:** 1489–1497

Friesen TL, Chu C, Xu SS, Faris JD (2012) SnTox5-*Snn5*: A novel *Stagonospora nodorum* effector-wheat gene interaction and its relationship with the SnToxA-*Tsn1* and SnTox3-*Snn3-B1* interactions. Mol Plant Pathol **13:** 1101–1109

Friesen TL, Holmes DJ, Bowden RL, Faris JD (2018) *ToxA* is present in the United States *Bipolaris sorokiniana* population and is a significant virulence factor on wheat harboring *Tsn1*. Plant Dis **102:** 2446–2452

Gao Y, Faris JD, Liu Z, Kim YM, Syme RA, Oliver RP, Xu SS, Friesen TL (2015) Identification and characterization of the SnTox6-*Snn6* interaction in the *Parastagonospora nodorum*-wheat pathosystem. Mol Plant Microbe Interact **28:** 615–625

Hane JK, Lowe RGT, Solomon PS, Tan KC, Schoch CL, Spatafora JW, Crous PW, Kodira C, Birren BW, Galagan JE, et al (2007) Dothideomycete plant interactions illuminated by genome sequencing and EST analysis of the wheat pathogen *Stagonospora nodorum*. Plant Cell **19:** 3347–3368

Haueisen J, Möller M, Eschenbrenner CJ, Grandaubert J, Seybold H, Adamiak H, Stukenbrock EH (2019) Highly flexible infection programs in a specialized wheat pathogen. Ecol Evol **9:** 275–294

IpCho SV, Tan KC, Koh G, Gummer J, Oliver RP, Trengove RD, Solomon PS (2010) The transcription factor StuA regulates central carbon metabolism, mycotoxin production, and effector gene expression in the wheat pathogen *Stagonospora nodorum*. Eukaryot Cell **9:** 1100–1108

Joehanes R, Nelson JC (2008) QGene 4.0, an extensible Java QTL-analysis platform. Bioinformatics **24:** 2788–2789

Jones JDG, Dangl JL (2006) The plant immune system. Nature **444:** 323–329

Kim D, Langmead B, Salzberg SL (2015) HISAT: A fast spliced aligner with low memory requirements. Nat Methods **12:** 357–360

Kosambi DD (1944) The estimation of map distances from recombination values. Ann Eugen **12:** 172–175

Li H, Handsaker B, Wysoker A, Fennell T, Ruan J, Homer N, Marth G, Abecasis G, Durbin R; 1000 Genome Project Data Processing Subgroup (2009) The sequence alignment/map format and SAMtools. Bioinformatics **25:** 2078–2079

Lin SY, Chooi YH, Solomon PS (2018) The global regulator of pathogenesis PnCon7 positively regulates *Tox3* effector gene expression through direct interaction in the wheat pathogen *Parastagonospora nodorum*. Mol Microbiol **109:** 78–90

Liu ZH, Faris JD, Meinhardt SW, Ali S, Rasmussen JB, Friesen TL (2004a) Genetic and physical mapping of a gene conditioning sensitivity in wheat to a partially purified host-selective toxin produced by *Stagonospora nodorum*. Phytopathology **94:** 1056–1060

Liu ZH, Friesen TL, Rasmussen JB, Ali S, Meinhardt SW, Faris JD (2004b) Quantitative trait loci analysis and mapping of seedling resistance to *Stagonospora nodorum* leaf blotch in wheat. Phytopathology **94:** 1061–1067

Liu Z, Friesen TL, Ling H, Meinhardt SW, Oliver RP, Rasmussen JB, Faris JD (2006) The *Tsn1*-ToxA interaction in the wheat-*Stagonospora nodorum* pathosystem parallels that of the wheat-tan spot system. Genome **49:** 1265–1273

Liu Z, Faris JD, Oliver RP, Tan KC, Solomon PS, McDonald MC, McDonald BA, Nunez A, Lu S, Rasmussen JB, et al (2009) *SnTox3* acts in effector triggered susceptibility to induce disease on wheat carrying the Snn3 gene. PLoS Pathog **5:** e1000581

Liu Z, Zhang Z, Faris JD, Oliver RP, Syme R, McDonald MC, McDonald BA, Solomon PS, Lu S, Shelver WL, et al (2012) The cysteine rich necrotrophic effector SnTox1 produced by *Stagonospora nodorum* triggers susceptibility of wheat lines harboring *Snn1*. PLoS Pathog **8:** e1002467

Liu Z, Gao Y, Kim YM, Faris JD, Shelver WL, de Wit PJGM, Xu SS, Friesen TL (2016) SnTox1, a *Parastagonospora nodorum* necrotrophic effector, is a dual-function protein that facilitates infection while protecting from wheat-produced chitinases. New Phytol **211:** 1052–1064

Lorieux M (2012) MapDisto: Fast and efficient computation of genetic linkage maps. Mol Breed **30:** 1231–1235

Love MI, Huber W, Anders S (2014) Moderated estimation of fold change and dispersion for RNA-seq data with DESeq2. Genome Biol **15:** 550

Lu S, Gillian Turgeon B, Edwards MC (2015) A ToxA-like protein from *Cochliobolus heterostrophus* induces light-dependent leaf necrosis and acts as a virulence factor with host selectivity on maize. Fungal Genet Biol **81:** 12–24

Manning VA, Ciuffetti LM (2015) Necrotrophic effector epistasis in the *Pyrenophora tritici-repentis*-wheat interaction. PLoS One **10:** e0123548

McDonald MC, Oliver RP, Friesen TL, Brunner PC, McDonald BA (2013) Global diversity and distribution of three necrotrophic effectors in *Phaeosphaeria nodorum* and related species. New Phytol **199:** 241–251

McDonald MC, Ahren D, Simpfendorfer S, Milgate A, Solomon PS (2018) The discovery of the virulence gene *ToxA* in the wheat and barley pathogen *Bipolaris sorokiniana*. Mol Plant Pathol **19:**432–439

Oliver RP, Friesen TL, Faris JD, Solomon PS (2012) *Stagonospora nodorum*: From pathology to genomics and host resistance. Annu Rev Phytopathol **50:** 23–43

Pertea M, Kim D, Pertea GM, Leek JT, Salzberg SL (2016) Transcript-level expression analysis of RNA-seq experiments with HISAT, StringTie and Ballgown. Nat Protoc **11:** 1650–1667

Pestsova E, Ganal MW, Röder MS (2000) Isolation and mapping of microsatellite markers specific for the D genome of bread wheat. Genome **43:** 689–697

Phan HTT, Rybak K, Furuki E, Breen S, Solomon PS, Oliver RP, Tan KC (2016) Differential effector gene expression underpins epistasis in a plant fungal disease. Plant J **87:** 343–354

Reddy L, Friesen TL, Meinhardt SW, Chao S, Faris JD (2008) Genomic analysis of the *Snn1* locus on wheat chromosome arm 1BS and the identification of candidate genes. Plant Genome **1:** 55–66

Richards JK, Wyatt NA, Liu Z, Faris JD, Friesen TL (2018) Reference quality genome assemblies of three Parastagonospora nodorum isolates differing in virulence on wheat. G3(Bethesda) **8:** 393–399

Röder MS, Korzun V, Wendehake K, Plaschke J, Tixier MH, Leroy P, Ganal MW (1998) A microsatellite map of wheat. Genetics **149:** 2007–2023

Rybak K, See PT, Phan HTT, Syme RA, Moffat CS, Oliver RP, Tan KC (2017) A functionally conserved Zn_2 Cys_6 binuclear cluster transcription factor class regulates necrotrophic effector gene expression and host-specific virulence of two major Pleosporales fungal pathogens of wheat. Mol Plant Pathol **18:** 420–434

SAS Institute (2011) SAS/STAT 9.3 User's Guide. SAS Institute Inc., Cary, NC

Shi G, Friesen TL, Saini J, Xu SS, Rasmussen JB, Faris JD (2015) The wheat *Snn7* gene confers susceptibility on recognition of the *Parastagonospora nodorum* necrotrophic effector SnTox7. Plant Genome-US **8:** 1–10

Shi G, Zhang Z, Friesen TL, Bansal U, Cloutier S, Wicker T, Rasmussen JB, Faris JD (2016a) Marker development, saturation mapping, and high-resolution mapping of the Septoria nodorum blotch susceptibility gene *Snn3-B1* in wheat. Mol Genet Genomics **291:** 107–119

Shi G, Zhang Z, Friesen TL, Raats D, Fahima T, Brueggeman RS, Lu S, Trick HN, Liu Z, Chao W, et al (2016b) The hijacking of a receptor kinase-driven pathway by a wheat fungal pathogen leads to disease. Sci Adv **2:** e1600822

Shirley MD, Ma Z, Pedersen BS, Wheelan SJ (2015) Efficient "pythonic" access to FASTA files using pyfaidx. PeerJ PrePRints **3:** e970v1

Somers DJ, Isaac P, Edwards K (2004) A high-density microsatellite consensus map for bread wheat (*Triticum aestivum* L.). Theor Appl Genet **109:** 1105–1114

Song QJ, Shi JR, Singh S, Fickus EW, Costa JM, Lewis J, Gill BS, Ward R, Cregan PB (2005) Development and mapping of microsatellite (SSR) markers in wheat. Theor Appl Genet **110:** 550–560

Sourdille P, Singh S, Cadalen T, Brown-Guedira GL, Gay G, Qi L, Gill BS, Dufour P, Murigneux A, Bernard M (2004) Microsatellite-based deletion bin system for the establishment of genetic-physical map relationships in wheat (*Triticum aestivum* L.). Funct Integr Genomics **4:** 12–25

Syme RA, Tan KC, Hane JK, Dodhia K, Stoll T, Hastie M, Furuki E, Ellwood SR, Williams AH, Tan YF, et al (2016) Comprehensive annotation of the *Parastagonospora nodorum* reference genome using next-generation genomics, transcriptomics and proteogenomics. PLoS One **11:** e0147221

Torada A, Koike M, Mochida K, Ogihara Y (2006) SSR-based linkage map with new markers using an intraspecific population of common wheat. Theor Appl Genet **112:** 1042–1051

van Schie CCN, Takken FLW (2014) Susceptibility genes 101: How to be a good host. Annu Rev Phytopathol **52:** 551–581

Virdi SK, Liu Z, Overlander ME, Zhang Z, Xu SS, Friesen TL, Faris JD (2016) New insights into the roles of host gene-necrotrophic effector interactions in governing susceptibility of durum wheat to tan spot and spetoria nodorum blotch. G3 (Bethesda) **6:** 4139–4150

Winterberg B, Du Fall LA, Song X, Pascovici D, Care N, Molloy M, Ohms S, Solomon PS (2014) The necrotrophic effector protein SnTox3 reprograms metabolism and elicits a strong defence response in susceptible wheat leaves. BMC Plant Biol **14:** 215

Xu SS, Friesen TL, Mujeeb-Kazi A (2004) Seedling resistance to tan spot and stagonospora nodorum blotch in synthetic hexaploid wheat. Crop Sci **44:** 2238–2245

Xue S, Zhang Z, Lin F, Kong Z, Cao Y, Li C, Yi H, Mei M, Zhu H, Wu J, et al (2008) A high-density intervarietal map of the wheat genome enriched with markers derived from expressed sequence tags. Theor Appl Genet **117:** 181–189

Zhang ZC, Friesen TL, Simons KJ, Xu SS, Faris JD (2009) Identification, development and validation of markers for marker-assisted selection against the *Stagonospora nodorum* toxin sensitivity genes *Tsn1* and *Snn2* in wheat. Mol Breed **23:** 35–49

Zhang Z, Friesen TL, Xu SS, Shi G, Liu Z, Rasmussen JB, Faris JD (2011) Two putatively homoeologous wheat genes mediate recognition of SnTox3 to confer effector-triggered susceptibility to *Stagonospora nodorum*. Plant J **65:** 27–38